

Leverage asymmetric strip tensions for enhanced control of surface roughness in skin-pass rolling

Mengmeng Zhang^{1*}, Christopher Schulte², Emad Scharifi¹, Sebastian Stemmler², David Bailly¹

¹Institute of Metal Forming (IBF), RWTH Aachen University, Aachen, Germany

²Institute of Automatic Control (IRT), RWTH Aachen University, Aachen, Germany

*E-mail: mengmeng.zhang@ibf.rwth-aachen.de

Abstract. In skin-pass rolling, ensuring uniform and precise strip surface roughness is essential, as the resulting strip roughness significantly influences tribological condition and paintability of semi-finished products. Therefore, to achieve the desired strip roughness in skin-pass rolling, this study proposes a control strategy for surface roughness using asymmetric strip tensions. For this purpose, a multiscale finite element model is employed to predict the strip roughness under variable thickness reductions, asymmetric tensions, initial strip roughness, and rolling speed. The results demonstrate that thickness reduction is the dominant factor influencing rolling force and surface roughness. Different combinations of asymmetric strip tensions adjust the strip roughness by up to 0.23 μm at 7% thickness reduction and 0.15 μm at 3% thickness reduction. The roughness adjustable range is obtained when the maximum achievable backward and forward tensions are 0.6 kN and 1.2 kN, respectively, for a 1.02 mm thick, and 8.06 mm wide strip. This highlights the potential to control strip roughness using asymmetric tensions. However, peak count of the strip surface remains unaffected by asymmetric tensions, and cannot be controlled in skin-pass rolling. Additionally, the effect of rolling speed is negligible when it exceeds 25 m min^{-1} at 3% thickness reduction. Furthermore, higher initial roughness contributes to a slight reduction in final strip roughness at 3% thickness reduction but has no impact at 7% thickness reduction. Validation results confirm the strong predictive capability of meso-model for roughness transfer behavior at variable thickness reductions and asymmetric tensions.

1 Introduction

The significance of surface roughness in industrial manufacturing cannot be overstated. For products such as bearings, minimizing friction is essential to facilitate relative movement between interfaces and reduce heat generation, necessitating a smooth surface [1]. However, for painted products, a rough surface improves paint adhesion between the coating and the substrate, thereby enhancing corrosion resistance [2]. In forming process such as deep drawing, inappropriate friction influenced by surface roughness leads to wrinkling [3], and significant springback behavior [4]. Therefore, it is necessary to adjust the roughness after the skin-pass rolling step to the desired product and customer demands.

Skin-pass rolling is conducted to obtain a desired surface topography, and improve surface flatness [5]. As the final step in cold rolling, it utilizes textured work rolls to transfer the topography of the roll surface onto the strip surface, described by the surface roughness transfer. However, thickness reduction in skin-pass rolling is found to have a significant effect on the resulting strip roughness. This is due to the fact that with increasing thickness reduction, deeper valleys will be formed on the strip surface, resulting



Content from this work may be used under the terms of the [Creative Commons Attribution 4.0 licence](#). Any further distribution of this work must maintain attribution to the author(s) and the title of the work, journal citation and DOI.

in a greater amount of material to form along the normal direction of the rolling process to fill valleys of the roll surface [6]. This phenomenon continues with increasing thickness reductions until the strip roughness reaches the limit of the roll surface roughness. This suggests that achieving the desired surface roughness while maintaining certain thickness reduction is challenging in skin-pass rolling because of the effect of the thickness reduction on the resulting strip roughness. Therefore, independently controlling both thickness reduction and surface roughness is difficult to be achieved in skin-pass rolling.

To ensure the desired strip roughness without influencing thickness reduction in skin-pass rolling, researchers have proposed two approaches. The first approach is fulfilled by the use of another roll stand, known as tandem rolling. The control strategy splits the total height reductions between the two roll stands with different work roll roughness, a method also referred to as adaptive pass scheduling. This approach enables the control of strip roughness R_a within a range of 1 μm to 2.5 μm at a constant thickness reduction of 8% when two set of work rolls with roughness $R_{a,roll}$ of 0.7 μm , and of 2.65 μm are used in two roll stands [7]. In terms of single-pass rolling, a control strategy utilizing symmetric strip tensions is introduced. It is concluded that with increasing strip tension, the roughness transfer ratio decreases at constant thickness reduction due to the decrease of the roll pressure. This demonstrates a high potential of applying different symmetric tensions to control the strip roughness and meanwhile ensure the geometric accuracy [8]. However, a disadvantage of this approach is that it requires high strip tensions, which increase further if the initial strip thickness deviates, to obtain a desired strip roughness.

Additionally, the effect of process parameters, such as rolling speed, and surface conditions on strip roughness should also be considered to ensure the control efficiency of different strategies in skin-pass rolling. Lubricants are widely used in industrial rolling mills, and several studies investigate the effect of the lubricant on roughness transfer. Compared to a dry surface condition, the use of lubricants reduces roughness transfer due to the formation of a film layer, and thus reduces the friction [9]. However, the presence of lubrication leads to a more homogeneous surface finish [10]. Additionally, the combined effect of surface condition and rolling speed is investigated in [11], showing that roughness transfer increases with increasing rolling speed under both dry and lubricated conditions. Under dry conditions, an increase in rolling speed raises the rolling force, thereby enhancing roughness transfer [10]. This effect is more dominant at lower rolling speeds [12]. However, under lubricated conditions, rolling speed has an even more pronounced effect. This is because the amount of lubricant entrapped in the strip surface valleys is dependent on the rolling speed [13].

In skin-pass rolling, the thickness reduction of the strip is a macroscopic phenomenon, while the deformation of surface peaks and valleys occurs at the microscopic or mesoscopic scale. Accurately capturing these multiscale deformations by a numerical method necessitates the use of highly refined meshes, which significantly increases computational costs and presents challenges for numerical studies [14]. To address this challenge, different finite element models are constructed. In [15] for example, a simplified finite element (FE) model for skin-pass rolling is constructed. The proposed model considers only the pure normal load of the roll, while neglecting the tangential shear stress between the roll and the strip. However, in skin-pass rolling, relative sliding occurs between the workpiece and the work roll in the slip zones. The resulting tangential shear stress has been shown to significantly influence the resulting surface roughness [16]. Furthermore, a multiscale modeling approach has been proposed to simulate surface roughness transfer in skin-pass rolling with improved efficiency. This approach models the rolling process at the macroscopic scale using a macro-model, while roughness transfer behavior is simulated at the mesoscopic scale using a meso-model [17]. It is found that this approach achieves high predictive accuracy for rolling force and the resulting strip roughness. Regular surface patterns of work rolls are preferred in multiscale models to reduce computational difficulty in FE simulations. For example in [8], an simple sinusoidal pattern of work rolls is used in the meso-model to predict the surface roughness. However, it overlooks the random contact nature of surface peaks, which affects the accuracy of surface roughness prediction.

This paper aims to investigate the influence of thickness reduction, strip tension, rolling speed, and initial strip roughness on the resulting strip roughness in skin-pass rolling through multiscale simulations, based on the previous work in [8]. The study accounts for the random contact characteristics between the roll and strip surface, and proposes a control strategy using asymmetric tensions to effectively achieve the desired roughness while considering the process parameters such as rolling speed and initial strip roughness.

2 Methodology

2.1 Materials and experimental setup

The skin-pass rolling experiments in this study utilize a two-high, single-pass rolling mill from Bühler Redex GmbH, based in Pforzheim, Germany. The mill is equipped with various sensors, including width and thickness gauges, as well as a laser-based roughness sensor from AMEPA GmbH, as shown in Figure 1.

These sensors continuously obtain the required data through laser-based measurements. The thickness gauges measure the incoming and outgoing thickness, while the width gauges record the incoming and outgoing width. The roughness sensor provides measurements of the surface mean roughness Ra and peak count RPc .

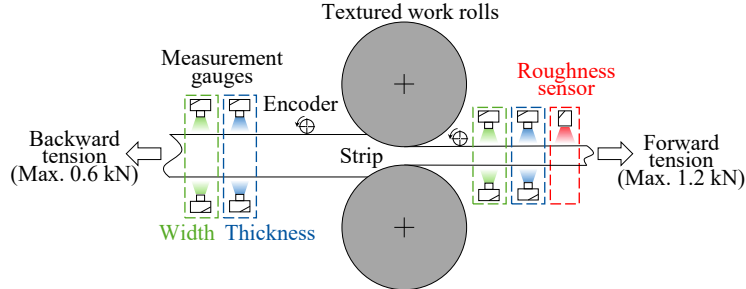


Figure 1: Experimental rolling mill equipped with encoders, thickness gauges (blue dashed box), width gauges (green dashed box), and a roughness sensor (red dashed box).

However, due to geometric limitations, the measurement sensor cannot be directly positioned within the roll gap, resulting in a measurement delay between the forming zone and the measurement. Therefore, an adaptive grey-box model was implemented to synchronize and estimate the measurements within the roll gap with the help of encoders, as detailed in [18, 19]. The roll gap height is controlled through the online adaptation of a developed roll stand deflection model and a cold rolling model to ensure precise outgoing thickness independent of material property changes or roll gap calibration errors, with further details provided in [20].

In this study, skin-pass rolling experiments were conducted using strips of cold-rolled low-carbon steel DC04 (1.0334, DIN EN 10130 [21]) with the strip width of 8.06 mm, and thickness of 1.02 mm. The work rolls are EDT-textured, exhibiting Ra_{roll} of 2.1 μm and RPc_{roll} of 80 cm^{-1} . The experiments are performed at the rolling speed of 5 m/min under dry surface conditions. Strip tensions are applied using the dancers of the cold rolling mill. The strip tension values are expressed in the unit of force rather than stress, as an experimental process parameter in this study. The experimental rolling mill, shown in Figure 1, allows for the maximum backward strip tension of 0.6 kN and the maximum forward strip tension of 1.2 kN.

2.2 Model setup

In skin-pass rolling, thickness deformation and surface formation occur at macroscopic and mesoscopic scales. To effectively capture both scales, a multiscale modeling approach is adopted in this study. A macro-model is used to simulate the rolling process in Abaqus/Standard 2019, with a detailed description available in a previous publication [8]. The meso-model, implemented in Abaqus/Explicit 2019, simulates the transfer of surface roughness from the roll to the strip surface. This section provides a comprehensive introduction to the meso-model.

2.2.1 Synthetic roll profile reconstruction. To predict the roughness transfer from the work roll to the strip surface, the surface profile of the roll needs to be incorporated into the meso-model. The experimental roll profile, represented by the black solid line in Figure 2, is derived using the replica method and then filtered according to ISO 21920-2 [22]. However, the inhomogeneity of the entire roll surface in experiments cannot be fully captured by a single surface profile with a sampling length of 2.5 mm. Furthermore, within different small sections of the 2.5 mm sampling length, the roughness values vary compared to the total roughness over 2.5 mm sampling length, leading to an inaccurate prediction of the resulting strip roughness if a specific range of 2.5 mm of the measured roll roughness is chosen. Hence, synthetic roll profiles are constructed by a sample generator based on the average of roughness values measured experimentally at different positions of roll surface. Furthermore, to simulate the random contact between the roll peaks and the strip, a Fourier series is used in the sample generator.

The developed sample generator systematically adjusts the mean roughness Ra , peak count RPc , and the Abbott-Firestone curve (AFC) to generate synthetic roll profiles that are equivalent to the experimental roll profile. A detailed description is available in a prepared publication [23]. The red solid

line in Figure 2 represents an example of a generated synthetic roll profile, which accurately reproduces the experimental profile in terms of average values of measured roughness parameters (Ra , RPC , and AFC) while maintaining a periodicity of 0.5 mm. This approach ensures that the generated profiles exhibit consistent roughness across different small sections, thereby achieving equivalence with the experimental roll profile.

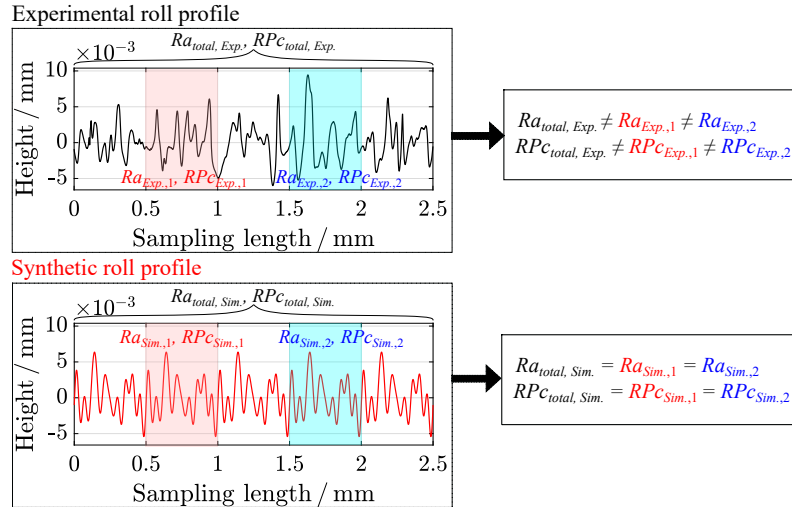


Figure 2: Roll profile comparison: the experimental profile is shown by the black solid line, while the synthetic profile is shown in red solid line.

2.2.2 Meso-model. The two-dimensional (2D) meso-model, presented in Figure 3, consists of two parts: the surface profile of the work roll and the workpiece. To achieve accurate roughness predictions, the roll curvature is considered based on the flattened radius used in the macro-model, which is estimated following the Hitchcock approach [24]. The workpiece length is set to 0.55 mm, with only the central 0.5 mm considered for roughness calculations due to the periodicity of the roll profile. The remaining 0.05 mm (0.025 mm on each side) is included to reduce computational errors caused by element distortion at the corners [23]. The meso-model operates under the plane strain assumption, neglecting the width spread. Moreover, only half of the strip is modeled, with the symmetry line located at the center of the strip thickness. The boundary conditions are derived from macro-model results, incorporating both stress field and roll kinematics. These inputs account for the effects of asymmetric strip tensions and the relative motion between the work roll and the strip in the meso-model. Therefore, effective coupling between the rolling process and roughness transfer behavior is achieved. A detailed description of these quantities can be found in [8]. A sensitivity study of the friction coefficient μ (0.10–0.40) shows a monotonic increase in the simulated rolling force by 1.0 kN, confirming the physical consistency of the model. Hence, μ is set to 0.36 in this study through inverse calibration in the macro-model to match the experimental rolling force.

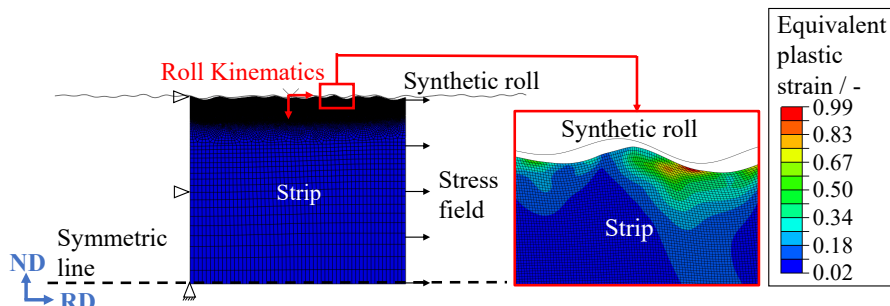


Figure 3: The meso-model set-up including the synthetic roll profile for predicting the roughness transfer, where the red square represents the equivalent plastic strain distribution.

3 Results and discussions

3.1 Numerical study

In this section, multiscale simulations are utilized to investigate the influence of process parameters on roughness transfer behavior, specifically the effects of asymmetric strip tensions (3.1.1), rolling speed (3.1.2), and initial strip roughness (3.1.3). Furthermore, the relative contributions of these process parameters to roughness transfer are analyzed. For the numerical study, synthetic roll profiles with $Ra_{roll} = 2.1 \mu\text{m}$ and $RPc_{roll} = 80 \text{ cm}^{-1}$ are generated and implemented in the meso-model.

3.1.1 Effect of asymmetric strip tension. To investigate the effect of asymmetric strip tensions, multiscale simulations are conducted under varying tension differences Δt , defined as the difference between the forward tension t_1 and the backward tension t_0 , given in (1). To maximize process asymmetry while staying within machine operational limits, the boundary conditions are defined as follows: when $\Delta t > 0$, $t_0 = 0.2 \text{ kN}$; when $\Delta t < 0$, $t_1 = 0.2 \text{ kN}$; and when $\Delta t = 0$, both t_0 and t_1 are set to 0.2 kN.

$$\Delta t = t_1 - t_0 \quad (1)$$

Figure 4 presents the macro- and meso-simulation results for rolling force, mean roughness Ra , and peak count RPc at thickness reductions of 3% and 7%. Notably, a part of the results, including the effect of asymmetric strip tension on rolling force and mean roughness Ra , is used in a prepared publication [23].

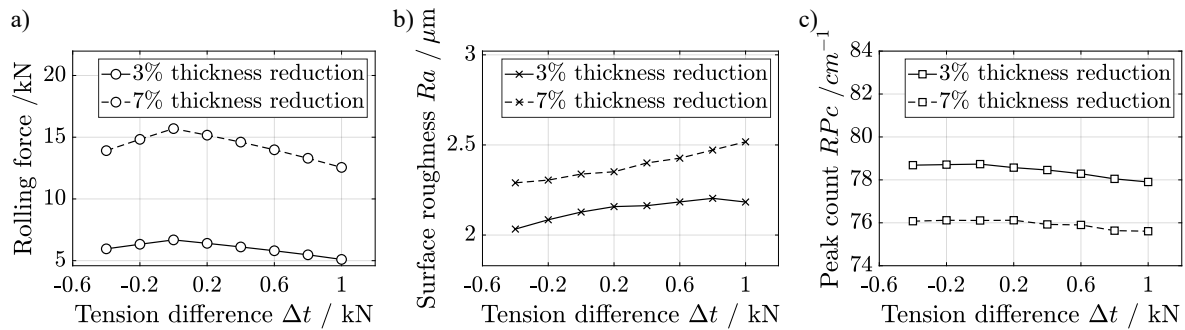


Figure 4: The effect of tension difference Δt at 3%, and 7% thickness reductions on: a) rolling force; b) mean roughness Ra ; c) peak count RPc . The simulations are conducted within the allowable operational range of Δt (from -0.4 kN to 1.0 kN), as constrained by the rolling mill.

As shown in Figure 4a, and Figure 4b, both rolling force and the resulting strip roughness Ra are influenced dominantly by the thickness reduction, in comparison to the effect of the tension difference Δt . For instance, the maximum achievable Ra at 3% thickness reduction (2.20 μm) remains lower than the minimum Ra attained at 7% thickness reduction (2.29 μm) within the operational machine limits of both tensions. Furthermore, roughness Ra continuously increases with increasing tension difference Δt from -0.4 kN to 1.0 kN. At 3% thickness reduction, Ra increases from 2.03 μm to 2.18 μm . At 7% thickness reduction, Ra increases from 2.29 μm to 2.52 μm . The detailed discussion is available in [23]. This variation in Ra at a constant thickness reduction suggests that asymmetric tensions can be utilized to achieve the desired Ra while maintaining the thickness reduction. However, the adjustable range is limited to 0.15 μm and 0.23 μm at 3% and 7% thickness reductions, respectively, for 1.02 mm thick and 8.06 mm wide DC04 material. These values correspond to conditions in which the maximum allowable backward tension is 0.6 kN and the maximum allowable forward tension is 1.2 kN, resulting in the Δt range from -0.4 kN to 1.0 kN.

To explore the potential for extending the adjustable range of Ra by increasing the range of tension difference Δt , a multiscale simulation is conducted at 3% thickness reduction with $\Delta t = -1.0 \text{ kN}$, using a backward tension of 1.2 kN and a forward tension of 0.2 kN. After that, the adjustable range of Ra is evaluated by calculating the roughness difference at the tension differences of $\Delta t = -1.0 \text{ kN}$ and 1.0 kN. Table 1 summarizes the comparison of Ra adjustable ranges before and after increasing the range of Δt . Notably, increasing the allowable backward tension to 1.2 kN expands the adjustable range of Ra from 0.15 μm to 0.32 μm , compared to the condition where the maximum allowable backward tension is 0.6 kN. These findings highlight the significant potential of asymmetric strip tension for roughness control in skin-pass rolling, provided that the adjustable range of strip tensions is sufficiently large.

In industrial skin-pass rolling, applicable strip tensions are significantly higher than those used in this study. The skin-pass mill at Thyssenkrupp Steel Europe (Dortmund, Germany) can apply maximum backward and forward tensions of 125 kN, while the skin-pass mill at Salem Steel Plant (Salem, India) allows strip tensions of up to 200 kN in both directions [25]. The minimum allowable strip width for both mills is 600 mm, corresponding to strip tensions per unit width of 208 N/mm and 333 N/mm, respectively. By contrast, the laboratory rolling mill used in this study applies a maximum forward tension of 1.2 kN and a backward tension of 0.6 kN to a strip with a width of 8.06 mm, resulting in 149 N/mm and 74.4 N/mm in the forward and backward directions, respectively. This substantial difference in operational tension limits suggests that an even wider adjustable range of surface roughness could be achieved under industrial conditions. Furthermore, from an operational perspective, the proposed strategy requires no additional hardware, as modern lines are equipped with high-performance tension motors. By adjusting the tension difference, roughness can be controlled without replacing the work rolls, thus offering a more cost-effective production process. In addition, compared to the symmetric tension-based strategy introduced in [8], the proposed asymmetric tension-based strategy enables more flexible control of surface roughness. Specifically, in the symmetric approach, roughness transfer is improved by reducing both forward and backward tensions. However, in industrial practice, the minimum allowable tension is constrained by flatness requirements and strip stability. In contrast, by increasing only forward tension, the roughness transfer can be enhanced in the asymmetric approach. This makes it a more practical and industrially feasible approach to roughness control in skin-pass rolling.

Table 1: Adjustable range of roughness Ra with an increased maximum allowable backward tension from 0.6 kN to 1.2 kN, while keeping the maximum allowable forward tension at 1.2 kN.

Tension Difference	Maximum Allowable Backward Tension t_0 / kN	Maximum Allowable Forward Tension t_1 / kN	Adjustable Ra Range / μm
Δt / kN			
-0.4 to 1.0	0.6	1.2	0.15
-1.0 to 1.0	1.2	1.2	0.32

However, Figure 4c shows that a higher thickness reduction of 7% results in a lower peak count RPc across all tension difference conditions compared to 3%, although the reduction remains below 3 cm^{-1} . This slight decrease is attributed to the increased strip elongation along RD at higher thickness reduction. According to ISO 21920-3, RPc is defined as the number of peaks per centimeter [26]. However, the initial strip length in the meso-model is only 0.5 mm, significantly shorter than the standard defined length. Hence, the number of peaks is normalized by the elongated strip length, which results in a lower computed RPc for the 7% thickness reduction.

In addition, the asymmetric strip tensions also do not show a significant effect on peak count RPc in this study. This is due to the fact that during skin-pass rolling, the formation of strip surface peaks is primarily determined by the characteristics of the work rolls, which have a peak count of $RPc = 80 \text{ cm}^{-1}$. Furthermore, it should be noted that the initial mean roughness Ra_0 and initial peak count RPc_0 of the strip are not considered in the numerical study presented in this section. Therefore, once RPc of the strip surface reaches the saturation level imposed by the roll surface profile, the formation of additional peaks is no longer possible. At thickness reduction of 3% and 7%, RPc of the strip surface is already approaching this saturation limit. Therefore, variations of the tension difference do not contribute to a change in RPc , as the roll surface profile inherently restricts peak formation, acting as the limitation of the roll profile. In this study, RPc cannot be controlled due to the negligible effect of tension difference Δt . In future work, the effect on RPc should be further investigated using work rolls with higher RPc . This can be achieved by optimizing the process parameters of EDT. For example, replacing conventional copper electrodes with graphite electrodes, or adopting positive-polarity pulse instead of capacitive discharge modes, enables more homogeneous discharge craters and higher RPc [27].

3.1.2 Effect of rolling speed. To investigate the influence of rolling speed on the resulting strip roughness, multiscale simulations are conducted at rolling speeds ranging from 5 m min^{-1} to 100 m min^{-1} under different tension differences ($\Delta t = -0.4 \text{ kN}$, 0.0 kN , and 1.0 kN) at 3% thickness reduction. The results are presented in Figure 5. When the rolling speed increases from 5 m min^{-1} to 100 m min^{-1} , an average increase of 1.18 kN in rolling force is observed in Figure 5a. Additionally, the mean roughness Ra exhibits a marginal average increase of $0.06 \mu\text{m}$ (Figure 5b). It can be noticed that the increasing rate of both rolling force and surface roughness reduces with increasing rolling speed. These findings are consistent with the results reported by [12].

To further analyze the effect of rolling speed, Figure 6 presents the slip ratio S_v and the normal pressure distribution within the contact area at $\Delta t = 0$ kN. As defined in (2), where v_{strip} and v_{roll} are the strip and roll velocities, respectively, S_v quantifies the relative motion between the strip and the roll.

$$S_v = \frac{v_{strip} - v_{roll}}{v_{roll}} \quad (2)$$

The x-axis represents the relative distance from the roll gap inlet, with $x = 0$ at the roll gap inlet and $x = 1$ at the outlet. As shown in Figure 6a, rolling speed does not affect the ratio of the sticking and slip zones. However, it affects the peak pressure within the contact region. As shown in Figure 6b, the peak pressure rises significantly from 3867 MPa to 4300 MPa until the rolling speed reaches 25 m min⁻¹, after which the increasing rate slows and stabilizes. This stabilization can be attributed to the saturation of dislocation density with increasing strain rate, and thus further increases in rolling speed no longer result in a significant increase in peak pressure. These observations suggest that the effect of rolling speed on the rolling force (Figure 5a), and strip roughness (Figure 5b) is driven by variations in peak pressure within the contact area due to the strain rate hardening.

In industrial skin-pass rolling, the rolling speed ranges from 50 to 1000 m/min [25]. The observed stabilization of strip roughness beyond 25 m/min indicates that the proposed roughness control strategy remains effective across this wide industrial speed range, confirming its practical applicability. However, when lubrication is introduced, this effect should be reconsidered, as rolling speed plays a crucial role in determining the amount of lubricant retained within surface valleys, and thus affects the tribological condition [13, 28].

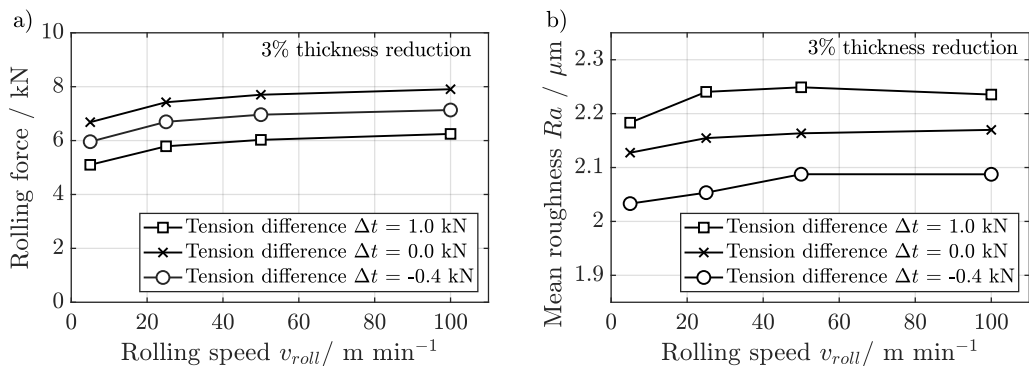


Figure 5: The influence of rolling speed from 5 m min⁻¹ to 100 m min⁻¹ at tension difference $\Delta t = -0.4$ kN, 0 kN, and 1.0 kN with thickness reduction of 3% on: a) rolling force; b) mean roughness Ra .

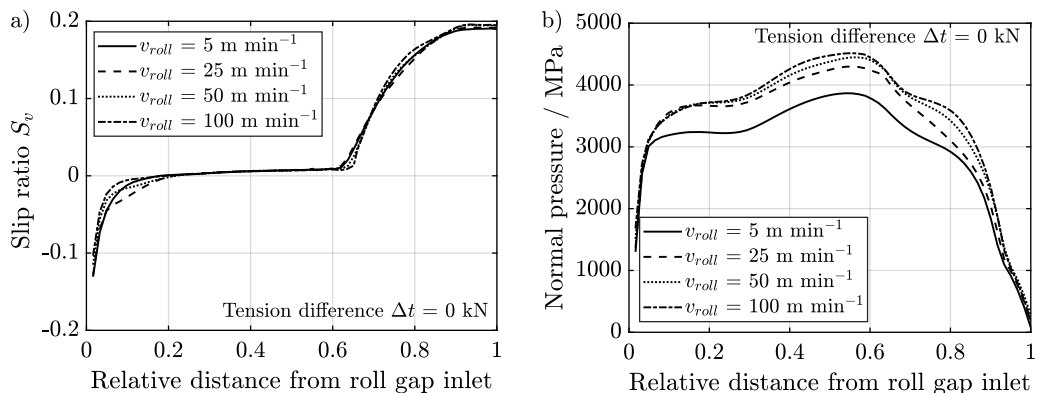


Figure 6: The influence of rolling speed from 5 m min⁻¹ to 100 m min⁻¹ at tension difference $\Delta t = 0$ kN with thickness reduction of 3% on the contact area regarding: a) relative velocity; b) normal pressure.

3.1.3 Effect of initial strip roughness. In the meso-model, the initial roughness Ra_0 , and initial peak count RPc_0 are included using a sinusoidal function. The amplitude corresponds to Ra_0 , and the wavelength is defined as $1/RPc_0$. The effect of the initial peak count RPc_0 is analyzed in Table 2, where the initial mean roughness Ra_0 is $1.4 \mu\text{m}$. The results show that when RPc_0 decreases from 110 cm^{-1} to 50 cm^{-1} , the resulting strip roughness Ra increases slightly by $0.09 \mu\text{m}$ at 3% thickness reduction. However, this effect becomes negligible at 7% reduction. Meanwhile, the resulting strip peak count RPc remains unaffected at both 3% and 7% thickness reductions.

Table 2: Influence of initial peak count RPc_0 on resulting roughness Ra and peak count RPc at tension difference $\Delta t = 0 \text{ kN}$ for 3% , and 7% thickness reductions.

Reduction	Initial roughness	Initial peak count	Final roughness	Final peak count
%	$Ra_0 / \mu\text{m}$	RPc_0 / cm^{-1}	$Ra / \mu\text{m}$	RPc / cm^{-1}
3	1.4	110	1.98	79.27
3	1.4	50	2.07	78.85
7	1.4	110	2.31	76.98
7	1.4	50	2.33	76.54

The effect of initial mean roughness Ra_0 on the resulting strip roughness Ra is evaluated in Figure 7a. An increase in Ra_0 from $0.5 \mu\text{m}$ to $1.4 \mu\text{m}$ while maintaining a constant RPc_0 of 110 cm^{-1} leads to a reduction in final roughness Ra by $0.12 \mu\text{m}$ at 3% thickness reduction. However, this effect is also negligible at 7% reduction. The pronounced effect of the initial roughness on the resulting Ra occurs at 3% thickness reduction because cold rolling is typically performed with smooth work rolls prior to skin-pass rolling, resulting in a relatively low Ra_0 . However, during skin-pass rolling, textured work rolls with higher roughness Ra_{roll} are employed. At higher thickness reduction of 7% , higher peaks form on the strip surface, which effectively override the initial roughness. In contrast, at lower thickness reduction of 3% , the effect of the initial roughness is dominant, as the newly formed low peaks and valleys are less dominant in modifying the initial strip roughness. When analyzing the effect of Ra_0 on the resulting strip peak count RPc in Figure 7b, the final peak count RPc is not significantly influenced. The difference is lower than 1 cm^{-1} at both 3% and 7% thickness reductions. This stability is attributed to the limited roll peak count RPc_{roll} of 80 cm^{-1} .

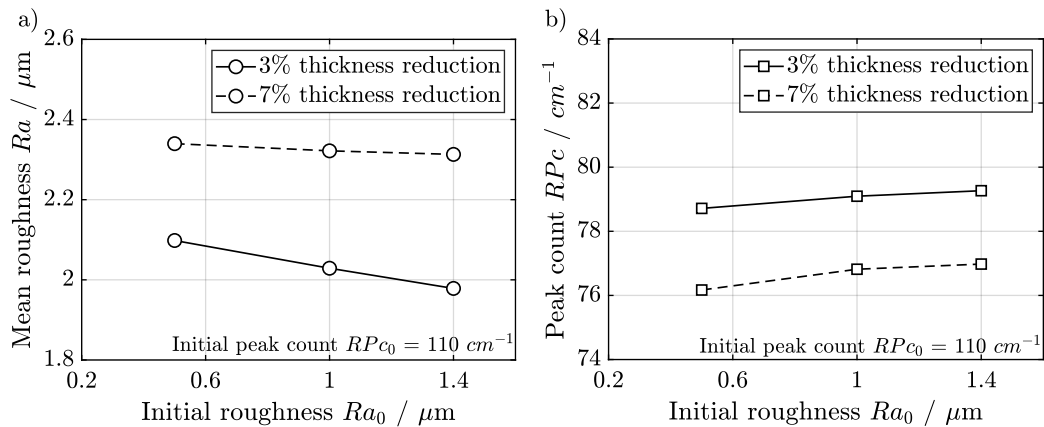


Figure 7: Effect of initial roughness Ra at tension difference $\Delta t = 0 \text{ kN}$ for 3% , and 7% thickness reductions: a) the effect on the strip mean roughness Ra ; b) the effect on the strip peak count RPc .

3.2 Validation of meso-model

Skin-pass rolling tests are conducted under varying thickness reductions and strip tensions to validate the multiscale model, with roughness continuously measured by the roughness sensor. Figure 8 compares the experimental and numerical results. Multiscale simulations are performed without considering the

initial strip roughness using four different roll surface profiles, all having an equivalent mean roughness R_{roll} of $2.1 \mu\text{m}$ and a peak count RPc_{roll} of 80 cm^{-1} .

The validity of the model at different deformation degrees is assessed by comparing simulations and experiments at thickness reductions of 3%, 5%, and 7% under a tension difference of $\Delta t = 0 \text{ kN}$ (Figure 8a). The resulting strip roughness, using four synthetic work rolls, constructs a confidence interval for the meso-model. It can be observed that the experimental measured mean roughness locates within the confidence interval for the meso-model predictions at 5% thickness reduction. However, at 3% and 7% thickness reductions, the measured mean roughness deviates slightly, likely due to numerical inaccuracy, such as an imprecise friction coefficient in the meso-model.

To further assess the model predictive capability under varying tension conditions, two asymmetric tension cases ($\Delta t = -0.4 \text{ kN}$ and 1.0 kN) at 5% thickness reduction are analyzed (Figure 8b). The meso-model demonstrates a high predictive accuracy, as the measured roughness remains within the confidence interval, confirming the robustness of the model in capturing the influence of strip tension on surface roughness.

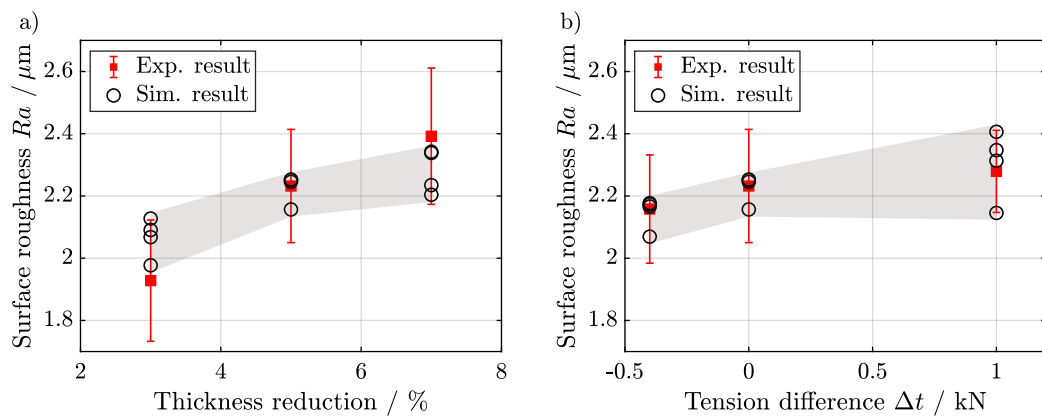


Figure 8: Experimental validation of the meso-model: a) for thickness reductions of 3%, 5%, and 7% at a tension difference of $\Delta t = 0 \text{ kN}$; b) for tension differences of $\Delta t = -0.4 \text{ kN}$ and $\Delta t = 1.2 \text{ kN}$ at thickness reduction of 5%.

4 Conclusion

The effects of asymmetric tension, rolling speed, and initial roughness on strip roughness are investigated using multiscale simulations. The meso-model is subsequently validated against skin-pass rolling tests. Based on this study, the following conclusions can be drawn:

- Thickness reduction is the primary factor influencing the rolling force and the resulting strip roughness R_a .
- In skin-pass rolling, asymmetric strip tensions can adjust the mean strip roughness R_a within a range of $0.23 \mu\text{m}$ at 7% reduction and $0.15 \mu\text{m}$ at 3% reduction when the maximum backward and forward tensions are 0.6 kN and 1.2 kN , respectively. Moreover, a case study at 3% height reduction with an increased maximum backward strip tension of 1.2 kN expands the adjustable range to $0.32 \mu\text{m}$. This suggests that asymmetric tension has the potential to control strip roughness R_a in skin-pass rolling, serving as an actuator, provided that the adjustable range of strip tensions is sufficiently large. However, the peak count RPc remains unaffected by asymmetric tensions because the roll profile has limited number of peaks.
- An increase in rolling speed initially leads to a slight rise in strip roughness R_a . However, beyond a certain point, the strip roughness R_a becomes unchanged.
- Higher initial strip roughness R_{a0} and peak count RPc_0 result in a slight reduction in the resulting roughness R_a at 3% reduction, but have no effect at 7% reduction due to the overriding influence of the roll profile, and higher peak formation at 7% reduction.
- The meso-model exhibits strong predictive capability for strip roughness R_a under various thickness reductions and strip tension conditions in skin-pass rolling.

To further broaden the applicability of roughness control, the influence of material variation on roughness transfer should be investigated in future work. Since the formation of surface peaks and valleys depends on the applied asymmetric tension and rolling force, materials with lower strength are more easily deformed under a given load. This may lead to enhanced roughness transfer in skin-pass rolling.

Conflict of Interest

The authors declare that they have no conflict of interest.

Acknowledgement

The authors gratefully thank to the funding by the Deutsche Forschungsgemeinschaft (DFG, German Research Foundation) – Project-ID 424333859 – within the SPP2183 on “Eigenschaftsgeregelte Umformprozesse”. A special thanks to Dr.-Ing. Stephan Hojda, and Xinyang Li for their contribution to the multi-scale modeling scheme for skin-pass rolling.

References

- [1] Bhattacharjee B, Chakraborti P and Choudhuri K 2020 *Tribologia - Finnish Journal of Tribology* **37** 13–25
- [2] Hagen C H M, Kristoffersen A and Knudsen ø 2016 *NACE CORROSION*
- [3] Reddy R V, Reddy T J and Reddy G C 2012 *International Journal of Engineering Trends and Technology* **3** 53–58
- [4] Dou S and Xia J 2019 *Metals* **9**
- [5] Kijima H 2014 *Journal of Materials Processing Technology* **214** 1111–1119
- [6] Nagase N, Shido S and Yarita I 2009 *ISIJ International* **49** 539–545
- [7] Schulte C, Li X, Stemmler S, Vallery H, Hirt G and Abel D 2023 *IFAC-PapersOnLine* **56** 2683–2688
- [8] Li X, Schulte C, Abel D, Teller M, Hirt G and Lohmar J 2021 *Advances in Industrial and Manufacturing Engineering* **3** 100045
- [9] Özakın B and Kurgan N 2021 *Arabian Journal for Science and Engineering* **46** 12137–12144
- [10] Çolak B and Kurgan N 2018 *The International Journal of Advanced Manufacturing Technology* **96** 3321–3330
- [11] Ma B, Tieu A, Lu C and Jiang Z 2002 *Journal of Materials Processing Technology* **125-126** 657–663
- [12] Simão J, Apinwall D K, Wise M L H and Subari K 1996 *Journal of Materials Processing Technology* **56** 177–189
- [13] Mekicha M A, de Rooij M B, Jacobs L, Matthews D and Schipper D J 2020 *Journal of Materials Processing Technology* **275** 116371
- [14] Wu C, Zhang L, Qu P, Li S, Jiang Z and Li W 2021 *Journal of Manufacturing Science and Engineering* **143**
- [15] Kijima H and Bay N 2008 *International Journal of Machine Tools and Manufacture* **48** 1313–1317
- [16] Kijima H and Bay N 2008 *International Journal of Machine Tools and Manufacture* **48** 1308–1312
- [17] Hojda S, Vogd M, Kang W, Pawelski H and Hirt G 2016 *10th International Rolling Conference and the 7th European Rolling Conference*
- [18] Schulte C, Li X, Abel D and Hirt G 2021 *IFAC-PapersOnLine* **54** 109–114
- [19] Wehr M, Stockert S, Abell D and Hirt G 2018 *IEEE Conference on Control Technology and Applications (CCTA)*
- [20] Wehr M, Stenger D, Schätzler S, Beyer R, Abel D and Hirt G 2020 *IFAC-PapersOnLine* **53** 10372–10379
- [21] Standard B 2006 *German version EN 10130*
- [22] ISO 21920-2 December 2022 *European Committee for Standardization*
- [23] Zhang M, Schulte C, Scharifi E, Stemmler S and Baily D 2025 Influence of asymmetric strip tension on surface roughness transfer in skin-pass rolling (in preparation)
- [24] Hitchcock J H 1935 *ASME Report of Special Research Committee on Roll Neck Bearings* **33** 33–41
- [25] SMS group 2020 Skin-pass mills for a perfect finish Brochure W6-318E San Donato Milanese, Italy
- [26] ISO 21920-3 December 2022 *European Committee for Standardization*
- [27] Tschersche S and Nitschke M 2012 *49th Rolling Seminar – Processes, Rolled and Coated Products* **49** 387–395
- [28] Emmens W C 1988 *15th Congress of International Deep Drawing Research Group (IDDRG)* 63–70